Focal bone defects in type 2 diabetes mellitus patients with acute hip fractures

Yuan, Y.; Zhang, R.; Yang, M.H.; Xia, W.; Su, Y.B.; Jian, J.M.; ... ; Wang, L.

Original Article

Focal bone defects in type 2 diabetes mellitus patients with acute hip fractures

Yi Yuan[1#], Rui Zhang[2#], Minghui Yang[3#], Wei Xia[2], Yongbin Su[4], Junming Jian[2], Yandong Liu[4], Zhe Guo[4], Xingyu Zhao[2], Shiwen Zhu[3], Xiaoguang Cheng[1,4], Xinbao Wu[3], Glen M. Blake[5], Annegreet Vlug[6], Klaus Engelke[7,8], Xin Gao[2], Ling Wang[1,4,9]

[1]Department of Radiology, Peking University Fourth School of Clinical Medicine, Beijing, China; [2]Medical Imaging Department, Suzhou Institute of Biomedical Engineering and Technology, Chinese Academy of Sciences, Suzhou, China; [3]Departments of Traumatic Orthopedics, Beijing Jishuitan Hospital, Capital Medical University, National Center for Orthopaedics, Beijing 100035, China; [4]Department of Radiology, Beijing Jishuitan Hospital, Capital Medical University, National Center for Orthopaedics, Beijing, China; [5]School of Biomedical Engineering & Imaging Sciences, King's College London, St Thomas' Hospital, London, United Kingdom; [6]Center for Bone Quality, Department of Internal Medicine, division of Endocrinology, Leiden University Medical Center (LUMC), Leiden, the Netherlands; [7]Department of Medicine 3, FAU University Erlangen-Nürnberg and Universitätsklinikum Erlangen, Erlangen, Germany; [8]Institute of Medical Physics, University Erlangen-Nürnberg, Germany; [9]JST Sarcopenia Research Center, Beijing Research Institute of Traumatology and Orthopaedics, Beijing 100035, China

Contributions: (I) Conception and design: Y Yuan, R Zhang, M Yang, X Cheng, X Wu, GM Blake, A Vlug, K Engelke, X Gao, L Wang; (II) Administrative support: X Cheng, X Wu, GM Blake, A Vlug, K Engelke, X Gao, L Wang; (III) Provision of study materials or patients: Y Yuan, R Zhang, M Yang, W Xia, Y Su, J Jian, Y Liu, Z Guo, X Zhao, S Zhu; (IV) Collection and assembly of data: Y Yuan, R Zhang, GM Blake, X Gao, L Wang; (V) Data analysis and interpretation: Y Yuan, Y Liu, Z Guo, L Wang; (VI) Manuscript writing: All authors; (VII) Final approval of manuscript: All authors.

[#]These authors contributed equally to this work as co-first authors.

Correspondence to: Ling Wang, PhD, MD. Department of Radiology, Peking University Fourth School of Clinical Medicine, Beijing, China; Department of Radiology, Beijing Jishuitan Hospital, Capital Medical University, National Center for Orthopaedics, No. 31 Xinjiekou East Street, Xicheng District, Beijing 100035, China; Sarcopenia Research Center, Beijing Research Institute of Traumatology and Orthopaedics, Beijing 100035, China. Email: doctorwl@bjmu.edu.cn; Xin Gao, PhD. Medical Imaging Department, Suzhou Institute of Biomedical Engineering and Technology, Chinese Academy of Sciences, 88 Keling Road, Suzhou 215163, China. Email: xingaosam@163.com.

Background: Osteoporotic hip fractures are associated with low bone strength, which is usually explained by low bone mineral density (BMD). However, even though type 2 diabetes mellitus (T2DM) participants have an increased incidence of osteoporotic hip fractures, paradoxically, there is increasing evidence indicating that T2DM patients have higher BMD than those without T2DM. The detection of focal osteoporosis could help us understand the bone quality of the proximal femur in participants with and without T2DM. This study aims to investigate whether focal bone defects are associated with hip fracture in those with and without T2DM by using statistical atlases.

Methods: Four hundred and nineteen low-energy acute hip fracture cases and 288 controls with hip computed tomography (CT) scans were included in the case-control study. Differences in the spatial distributions of volumetric bone mineral density (vBMD), cortical bone thickness, cortical vBMD, and vBMD in a layer adjacent to the endosteal surface were investigated using voxel-based morphometry (VBM) and surface-based statistical parametric mapping (SPM).

Results: For both with and without T2DM groups, there is a clear bone defect at the femoral neck and intertrochanteric region in cortical thickness variables for cases. The endocortical trabecular bone mineral density (ECTD) and vBMD distributions show quite dramatic differences between fractures and controls in both with and without T2DM groups. In particular, in the women's comparison results, the significantly

different region between cases and controls in the T2DM cohort was larger than that in the without T2DM cohort. After adjustment for the covariates of age, height, and weight, the risk of hip fracture among people with diabetes was higher overall than among participants without diabetes, in both men and women. The spatial distribution of trabecular vBMD and focal areas of endocortical bone defect both result in an increased risk of hip fracture in T2DM patients.

Conclusions: The spatial distribution of trabecular vBMD and focal areas of endocortical bone defect both result in increased risk of hip fracture in T2DM patients.

Keywords: Acute hip fracture; voxel-based morphometry (VBM); statistical parametric mapping (SPM); bone mineral density (BMD); type 2 diabetes mellitus (T2DM)

Submitted Mar 05, 2025. Accepted for publication Aug 13, 2025. Published online Sep 11, 2025.
doi: 10.21037/qims-2025-560
View this article at: https://dx.doi.org/10.21037/qims-2025-560

Introduction

In ageing societies, type 2 diabetes mellitus (T2DM) and osteoporosis are common metabolic diseases whose prevalence is increasing throughout the world (1,2). The complications of diabetes affect multiple organ systems, including bone. Osteoporotic fractures are associated with low bone strength, which is usually explained by low bone mineral density (BMD). However, there is increasing evidence from recent studies consistently indicating that T2DM patients have higher or equivalent BMD compared to those without T2DM. The increase in BMD was more prominent in the presence of higher body mass index (BMI) in T2DM patients and obesity, as a strong risk factor for T2DM, would protect against osteoporosis (3-7). Paradoxically, T2DM prevalence has been linked to increased fracture risk and an increased incidence of osteoporotic fractures (3,8,9). This contradiction may be caused by damage to bone microstructure or an accumulation of microcracks that reflect sustained impairment of bone repair (10,11).

Hip fractures are the most severe osteoporotic fractures in the elderly, with a high degree of morbidity, mortality, and disability. Due to the complications of diabetes mellitus, T2DM participants with hip fractures are expected to have higher mortality and disability than hip fracture patients without T2DM. Advanced imaging techniques to assess bone quality have only recently started to be applied in clinical practice. Further, the assumption of poor bone quality in T2DM patients might not apply to the proximal femur as most studies have been limited to appendicular bones assessed by high-resolution peripheral quantitative computed tomography (HR-pQCT) (12-14). Computational anatomy techniques such as surface-based statistical parametric mapping (SPM) and voxel-based morphometry (VBM) enable local multiparametric assessments of the spatial distribution of volumetric bone mineral density (vBMD) and structural features of the proximal femur to be derived from quantitative computed tomography (QCT) imaging of sufficiently large populations. SPM was a methodology that has its roots in neuroimaging and has been used to identify focal osteoporosis affecting trabecular and cortical bone of the proximal femur in hip fractures (15). Carballido-Gamio *et al.* applied VBM to identify femoral regions where bone deterioration has been associated with incident hip fracture (16). Treece *et al.* also demonstrated the application and validation of the method (17). The detection of focal osteoporosis by SPM and VBM could help us understand the bone quality of the proximal femur in participants with and without T2DM. To the best of our knowledge, no study has used statistical atlases to identify differences of the proximal femur between hip fracture patients with and without T2DM, as well as between controls without hip fractures with T2DM and without T2DM.

The study aimed to investigate if there are focal bone defects of the proximal femur in T2DM and whether focal bone defects are associated with hip fracture. For this purpose, we used data from the China Action on Spine and Hip Status (CASH) study, including controls without hip fracture. We identified the differences in the spatial distributions of proximal femoral vBMD and cortical bone properties across groups of T2DM participants with and without hip fractures as compared with controls without T2DM using VBM and SPM. We present this article in

accordance with the STROBE reporting checklist (available at https://qims.amegroups.com/article/view/10.21037/qims-2025-560/rc).

Methods

Study design

The CASH study aims to assess the prevalence of osteoporotic fracture, osteoporosis, and osteoarthritis (OA) in a Chinese population using QCT and/or dual energy X-ray absorptiometry (DXA) (18). The study was conducted in accordance with the Declaration of Helsinki and its subsequent amendments. The study was approved by institutional ethics committee of Beijing Jishuitan Hospital (No. 201512-02) and informed consent was taken from all the participants. The present analysis compared computed tomography (CT) scans of hip fracture patients acquired immediately after injury with CT images obtained from controls without hip fractures. In this case control study, we explored spatial and structural features of the proximal femur for the discrimination of diabetic hip fracture as well as non-fracture diabetes and without diabetes mellitus participants.

Participants

The study enrolled 918 participants with suspected hip fracture admitted to the Emergency Department of Orthopedic Trauma in Beijing Jishuitan Hospital between January 2012 and May 2016. At this institution, CT scans are performed routinely for participants with suspected or already confirmed hip fractures. The demographic data, details of the fall (when, how, where), fracture history, and medical history were collected after the CT examination. The inclusion and exclusion criteria of the participants were previously described by Su and colleagues (19). In brief, fully ambulatory, community-dwelling Chinese adults with a hip fracture resulting from a fall from standing or sitting height were included. Furthermore, CT scans were obtained within 48 hours of falls to minimise changes in vBMD and body composition caused by bedrest after fracture. Participants with prior or bilateral hip fractures were excluded. Finally, 419 hip fracture cases were considered eligible for further analysis. Diabetes diagnosis and related treatment were derived from the medical records, which also confirmed there were no type 1 diabetics among the fracture cases.

As controls, 288 community-dwelling participants without hip fracture and living independently were recruited from the hospital's neighborhood. The inclusion criteria are that participants should be aged over 60 years old and able to give informed consent. All the participants underwent QCT scans of the lumbar spine and hip. The exclusion criteria for the control participants were inability to sit and stand independently or inability to walk with or without an assistive device. Further exclusion criteria for both groups were diseases that limited function, i.e., stroke, neurologic disorders, rheumatic diseases, heart failure, and others (20). Diabetes diagnosis and related treatment were retrieved from the control participants' medical profiles in the Xinjiekou Community Health Service Center.

A flowchart containing stepwise inclusion and exclusion of the participants is shown in *Figure 1*.

CT acquisition

Spiral CT imaging of the hip was performed for all participants with two Toshiba Aquilion CT scanners (Toshiba Medical Systems Division, Tokyo, Japan). The scan range was from the top of the acetabulum to 3 cm below the lesser trochanter (TR) and included both legs. A Mindways calibration phantom (Mindways Software Inc., Austin, TX, USA) was placed beneath each participant's hips. Measurements were made on the intact contralateral femur of the participants with hip fracture and the right proximal femur of the controls. The acquisition parameters were: 120 kVp, 125 mAs, 50 cm field of view, 512×512 matrix, 1 mm reconstructed slice thickness, and a standard reconstruction kernel.

BMD

Areal BMD (aBMD, g/cm^2) and vBMD (mg/cm^3) of the femoral neck (FN), TR, intertrochanter (IT) and total hip (TH) were calculated by the computed tomography X-ray absorptiometry technique (CTXA, version 4.2.3, Mindways Inc.). CTXA is a DXA-equivalent technique and the aBMD measures obtained by CTXA are in good agreement with DXA (21). The Femur option of the Medical Image Analysis Framework software (MIAF Femur Version 7.1.0MRH) was used to segment the proximal femur from the surrounding soft tissue as well as the cortical and trabecular bone (22). The masks generated from MIAF were used for further imaging process. Based on the calibration phantoms, Hounsfield units (HU) were converted to equivalent density

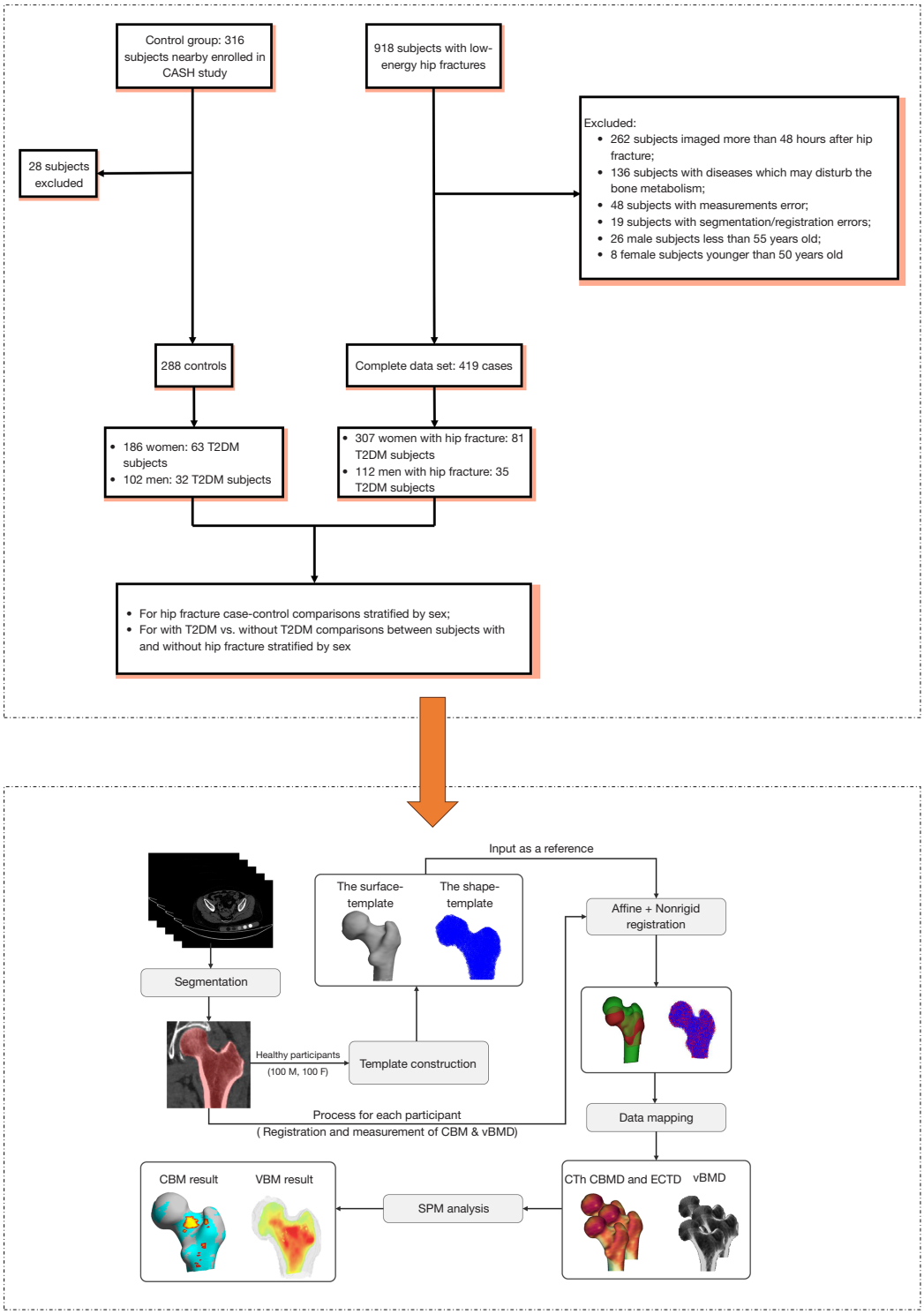

Figure 1 Flow diagram of participants selection and the CBM and VBM technique. All images were segmented and bone properties (cortical bone properties and vBMD) were calculated. Using the registration method, all scans in the study were spatially normalized to a standardized template. Surface-based SPM analysis was used to identify spatial differences in bone properties between cases and controls. CBM, cortical bone mapping; ECTD, endocortical trabecular bone mineral density; SPM, statistical parametric mapping; T2DM, type 2 diabetes mellitus; VBM, voxel-based morphometry; vBMD, volumetric bone mineral density.

of calcium hydroxyapatite in anonymized scans. Precision results of endocortical trabecular bone mineral density (ECTD) and vBMD measurements have been published earlier (23). Our methods were in accordance with established protocols from the previous study. To ensure the repeatability of measurements, all the measurements were performed by the same observer. To assess variability, two observers evaluated scans for 20 images 2 weeks later. Inter- and intra-observer variability were good (intraclass correlation coefficients >0.80).

Image preprocessing

Standard template construction

In this study, 100 males and 100 females from the healthy controls were used to construct the corresponding standard template. The right proximal femur was selected and segmented for all the healthy controls. Two types of standard template were constructed to provide a template appropriate to the population sample, one to represent the average femur surface (the surface-template), and a second one to represent the average shape and internal structure of the proximal femur (the shape-template). The standard template was previously described by Carballido-Gamio and colleagues (16).

Stradwin software (http://mi.eng.cam.ac.uk/~rwp/stradwin) excels at efficiently generating smooth and accurate surface models from 3D medical images. Thus, we used it specifically for this strength to construct the surface template. For the surface-template, Stradwin software was used to create a regular proximal femoral surface mesh based on the segmented proximal femur for all the participants with between 6,000 and 11,000 vertices distributed over the proximal femoral surface for each participant. A participant was selected as the initial template. We then registered this template to each participant, producing 200 nonrigid transformations (100 males and 100 females). From these, we computed a mean transformation and warped the initial image using the mean transformation to produce a new template. We then registered this new template to each participant and warped the template using the corresponding transformation. The resulting image was the output template for this iteration, which then became the input for the next iteration. This procedure was repeated until no further changes were made to the mean template. In this way, the surface-templates based on the male and female image data were finally constructed.

Matrix Laboratory (MATLAB) provides a powerful and flexible environment for these matrix-based computations and custom algorithms. For the shape-template, MATLAB and the Coherent Point Drift (CPD) algorithm (24) were used. For the shape-template, MATLAB and the CPD algorithm (24) were used. Firstly, point clouds for 200 participants were created with between 10,000 and 13,000 points distributed in the proximal femur of each participant, and one of the point clouds was selected as the initial template. The CPD algorithm (including an affine transformation and a nonrigid transformation) was used to register the remaining point clouds to the initial template. Then, an iterative procedure similar to the construction of the surface-template was performed, the resulting average coordinate space representing the final shape-template.

Cortical bone mapping (CBM) and VBM

The CBM and VBM pipeline are summarized in *Figure 1*, and described in more detail below.

To perform CBM, the first step was to create a regular proximal femoral surface mesh based on the segmented proximal femur (17) and obtain CBM measurements for each vertex of the surface mesh using the Stradwin software. The CBM measurements included cortical thickness (CTh, mm), cortical mass surface density (CM, mg/cm^2), cortical bone mineral density (CBMD, mg/cm^3), and ECTD (mg/cm^3). The proximal femoral surface mesh was registered to the surface-template and the CBM measurements were mapped to that average surface-template using wxRegSurf (http://mi.eng.cam.ac.uk/~-ahg/wxRegSurf/).

To perform VBM, the first step was to create a regular point cloud based on all the segmented proximal femur image data, and all the point clouds were spatially registered to the shape-template using the CPD registration method (25). Then, a 4-mm full-width at half-maximum (FWHM) Gaussian kernel was used to smooth the spatially normalized image to ensure that each voxel represented the average vBMD from its local neighborhood, and the average vBMDs were mapped to the average shape-template.

Data collection

Demographic and anthropometric variables included age, gender, and BMI. Health-related data included a history of hypertension, coronary heart disease, OA, and previous fractures.

Statistical analysis

Statistical analysis was conducted using R software (version 3.5.1, https://www.r-project.org/). Participant characteristics (age, height, weight, aBMD, and vBMD) were compared and expressed as mean and standard deviation using the Mann-Whitney *U* test to determine the significance of any differences between cases and controls. A P value smaller than 0.05 was considered statistically significant.

The general linear model (GLM) in SPM was applied to identify differences in any of the CBM measurements between cases and controls using the SurfStat package (http://www.stat.uchicago.edu/~worsley/surfstat/poster.htm). The co-variables used in GLM were the participant characteristics and model shape. Only negative residuals are plotted in the figures, and the small number of positive residuals caused by statistical noise were ignored. Missing height and weight values were replaced with group mean values. In the male populations, there were 11 missing weight values and 9 missing height values. There were 16 missing weight values and 13 missing height values in the female populations. The five most significant shape modes were used to account for any systematic misregistration during the registration process, and model shape mode 1 (femur size) was not included in the GLM because it would reduce the fracture-sensitive results (26). A voxel-wise GLM was performed in VBM analysis to identify differences of vBMD between cases and controls. The vBMD values at each voxel location were used as the dependent variable, and age, height, and weight were included as co-variables in the vBMD comparisons. The age-matched controls cohort was designed to reduce the imbalance between fracture cases and controls without T2DM in the female population.

In addition, patches with significant differences between cases and controls in CBM and vBMD were identified. To investigate the effect of T2DM on focal bone, odds ratios (ORs) were calculated for each variable individually using binomial logistic regression, including aBMD and vBMD values, CBM patches, and vBMD patches after adjustment for the base covariates (age, height, and weight).

Results

Participant characteristics

The participant characteristics including the mean (± standard deviation) of the age, height, weight, aBMD and vBMD in male and female populations are listed in *Table 1*. Generally, there were significant difference in all characteristics between hip fracture and control cohorts with or without T2DM (the male or female populations) except for height and history of previous fractures. Compared with the control cohorts, fracture cohorts had lower aBMD and vBMD in male and female populations.

SPM analysis of different bone properties

Figures 2,*3* illustrate these comparisons for males and females, respectively, and the detailed numerical outcomes for these spatially significant patches were summarized in *Table 2*. Significant regional variations in bone characteristics between the fracture and control groups were found by the SPM analysis, which was conducted independently with and without T2DM cohorts.

In males, the T2DM and without T2DM groups had a distinct patch at the FN and intertrochanteric area in CTh variables (*Figure 2A*). In CBMD variables, comparison results showed relatively greater differences compared to the other CBM variables. In male with T2DM group, the significant CBMD differences were primarily observed in the region of the femoral head, the greater TR and the lesser TR, but CBMD results showed no significant differences in these regions in male without T2DM group (*Figure 2B*).

In females, there is a clear patch at the FN and intertrochanteric region between T2DM and without T2DM groups in CTh variables (*Figure 3A*). The variations in CBMD distributions in female populations indicate that the groups with and without T2DM are similar (*Figure 3B*). In particular, the significantly different region between cases and controls in the T2DM cohort was larger than that in the group without T2DM (*Figure 3C*,*3D*).

Figure 4 shows the focal defects in bone are similar to the outcomes in *Figures 2*,*3*.

ORs

Figure 5 displays the ORs for the male and female populations. In both the male and female groups, the total risk of hip fracture was greater for participants with T2DM than for those without the disease, even after controlling for age, height, and weight.

Discussion

To our knowledge, this is the first study examining spatial differences in proximal femoral bone density and cortical

Table 1 Characteristics of participants

Characteristics	Hip fracture patients		Controls		P values	
	With T2DM [1]	Without T2DM [2]	With T2DM [3]	Without T2DM [4]	[1] *vs.* [3]	[2] *vs.* [4]
Male						
Sample size	35	77	32	70	–	–
Age (years)	75.8±8.1	74.5±9.4	68.6±6.2	67.3±7.5	<0.05	<0.05
Height (cm)	171.2±5.3	171.2±5.7	170.3±5.2	170.7±5.3	0.684	0.802
Weight (kg)	74.0±21.1	66.6±11.0	73.9±11.1	72.9±9.5	0.477	<0.05
BMI (kg/m^2)	25.40±8.49	22.71±3.35	25.39±3.02	24.97±2.66	0.248	<0.05
Hypertension	5.71 [2]	18.19 [14]	–	–	–	–
History of CHD	0 [0]	3.90 [3]	–	–	–	–
OA	2.86 [1]	10.39 [8]	–	–	–	–
History of previous fractures	5.71 [2]	23.38 [18]	25.00 [8]	10.00 [7]	0.026	0.031
TH aBMD (g/cm^2)	0.7±0.1	0.7±0.1	0.9±0.2	0.9±0.1	<0.05	<0.05
TH BMD (mg/cm^3)	218.8±34.6	221.8±42	294.6±50.7	290.5±48.8	<0.05	<0.05
FN aBMD (g/cm^2)	0.6±0.1	0.6±0.1	0.7±0.1	0.7±0.1	<0.05	<0.05
FN BMD (mg/cm^3)	215.3±43.9	219.7±40.5	290.5±55.3	292.4±58.3	<0.05	<0.05
TR aBMD (g/cm^2)	0.5±0.1	0.5±0.1	0.6±0.1	0.6±0.1	<0.05	<0.05
TR BMD (mg/cm^3)	140.4±30.1	144.1±31.4	201.3±40.6	197.4±37.4	<0.05	<0.05
IT aBMD (g/cm^2)	0.8±0.1	0.8±0.1	1.1±0.2	1.1±0.2	<0.05	<0.05
IT BMD (mg/cm^3)	271.1±44.9	270.6±52.4	358.1±60.3	351.5±60.3	<0.05	<0.05
Female						
Sample size	81	226	63	123	–	–
Age (years)	74.9±8.5	75.0±9.2	68.7±6.0	65.2±6.1	<0.05	<0.05
Height (cm)	158.9±5.0	158.1±5.4	157.9±5.5	158.7±5.3	0.108	0.256
Weight (kg)	61.1±9.2	58.3±10.2	65.5±9.7	62.9±9.5	<0.05	<0.05
BMI (kg/m^2)	23.86±4.43	23.29±3.76	26.18±3.26	24.91±3.17	<0.05	<0.05
Hypertension	17.73 [14]	18.42 [42]	–	–	–	–
History of CHD	6.32 [5]	7.01 [16]	–	–	–	–
OA	6.32 [5]	13.60 [31]	–	–	–	–
History of previous fractures	22.78 [18]	18.42 [42]	22.22 [14]	20.32 [25]	0.840	0.693
TH aBMD (g/cm^2)	0.6±0.1	0.6±0.1	0.8±0.2	0.7±0.2	<0.05	<0.05
TH BMD (mg/cm^3)	213.3±42.4	207.1±41.5	282.5±57.3	272.2±83.8	<0.05	<0.05
FN aBMD (g/cm^2)	0.5±0.1	0.5±0.1	0.7±0.1	0.6±0.2	<0.05	<0.05
FN BMD (mg/cm^3)	226.7±42.8	217.7±42.5	312.5±70.2	296.7±95.9	<0.05	<0.05
TR aBMD (g/cm^2)	0.4±0.1	0.4±0.1	0.5±0.1	0.5±0.2	<0.05	<0.05
TR BMD (mg/cm^3)	130.4±29.3	128.6±31	186.3±40	179.9±57.6	<0.05	<0.05
IT aBMD (g/cm^2)	0.7±0.1	0.7±0.1	0.9±0.2	0.9±0.3	<0.05	<0.05
IT BMD (mg/cm^3)	259.5±54.8	250.9±52.5	342.4±70.7	327.2±101.9	<0.05	<0.05

Data are expressed as mean ± standard deviation, n or % [n]. aBMD, areal bone mineral density; BMI, body mass index; CHD, coronary heart disease; FN, femoral neck; IT, intertrochanter; OA, osteoarthritis; TH, total hip; T2DM, type 2 diabetes mellitus; TR, trochanter.

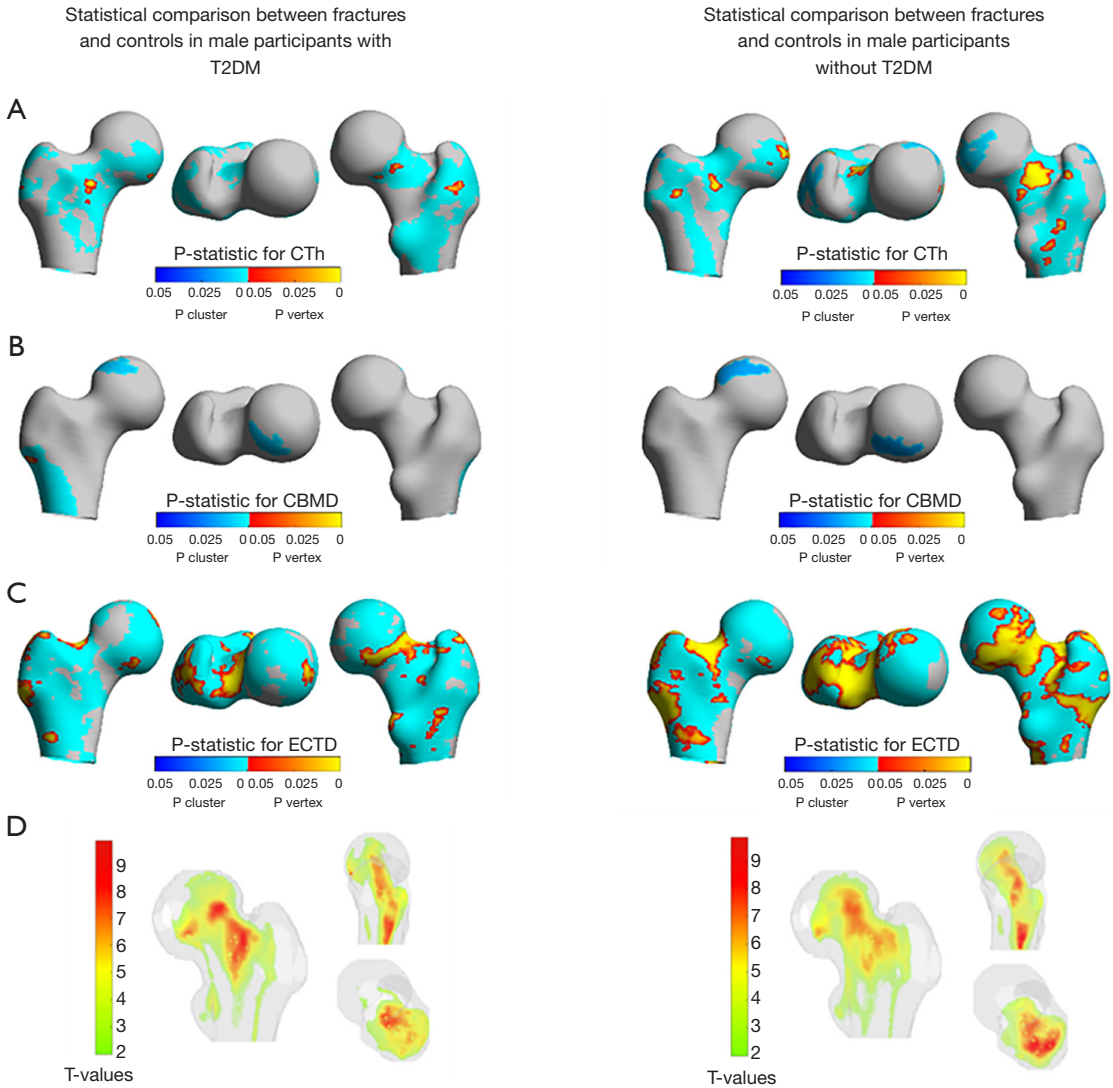

Figure 2 Comparisons of different bone properties between male hip fractures and controls with and without T2DM. The left-hand images were derived from participants with T2DM and the right-hand images were derived from participants without T2DM. (A) SPM T-maps from CTh comparisons; (B) SPM T-maps from CBMD comparisons; (C) SPM T-maps from ECTD comparisons; (D) VBM T-maps from vBMD comparisons. In parts A, B and C of these figures, the P-vertex results (yellow-orange colour map) show P values for vertex peaks, and the P-cluster results (cyan-blue colour map) show P values of connected clusters that exceed a P value threshold of 0.05. The color scale in D is based on the dynamic range of Student's *t*-values, where nonsignificant voxels have been rendered transparent and significant voxels assigned a degree of opacity based on its *t*-value. CBMD, cortical bone mineral density; CTh, cortical thickness; ECTD, endocortical trabecular bone mineral density; SPM, statistical parametric mapping; T2DM, type 2 diabetes mellitus; VBM, voxel-based morphometry.

bone properties in participants with T2DM in relation to hip fracture. Our results identified acute hip fracture related features of T2DM patients using VBM analysis of vBMD and SPM analysis of cortical bone properties, thus providing a more comprehensive QCT assessment of the proximal femur. VBM and SPM results suggest that the spatial distribution of trabecular vBMD, as well as focal areas of cortical and endocortical bone defects, might play a significant role in increased hip fracture risk for T2DM patients.

Although participants with T2DM have an excessive risk of hip fracture compared with without T2DM group, the

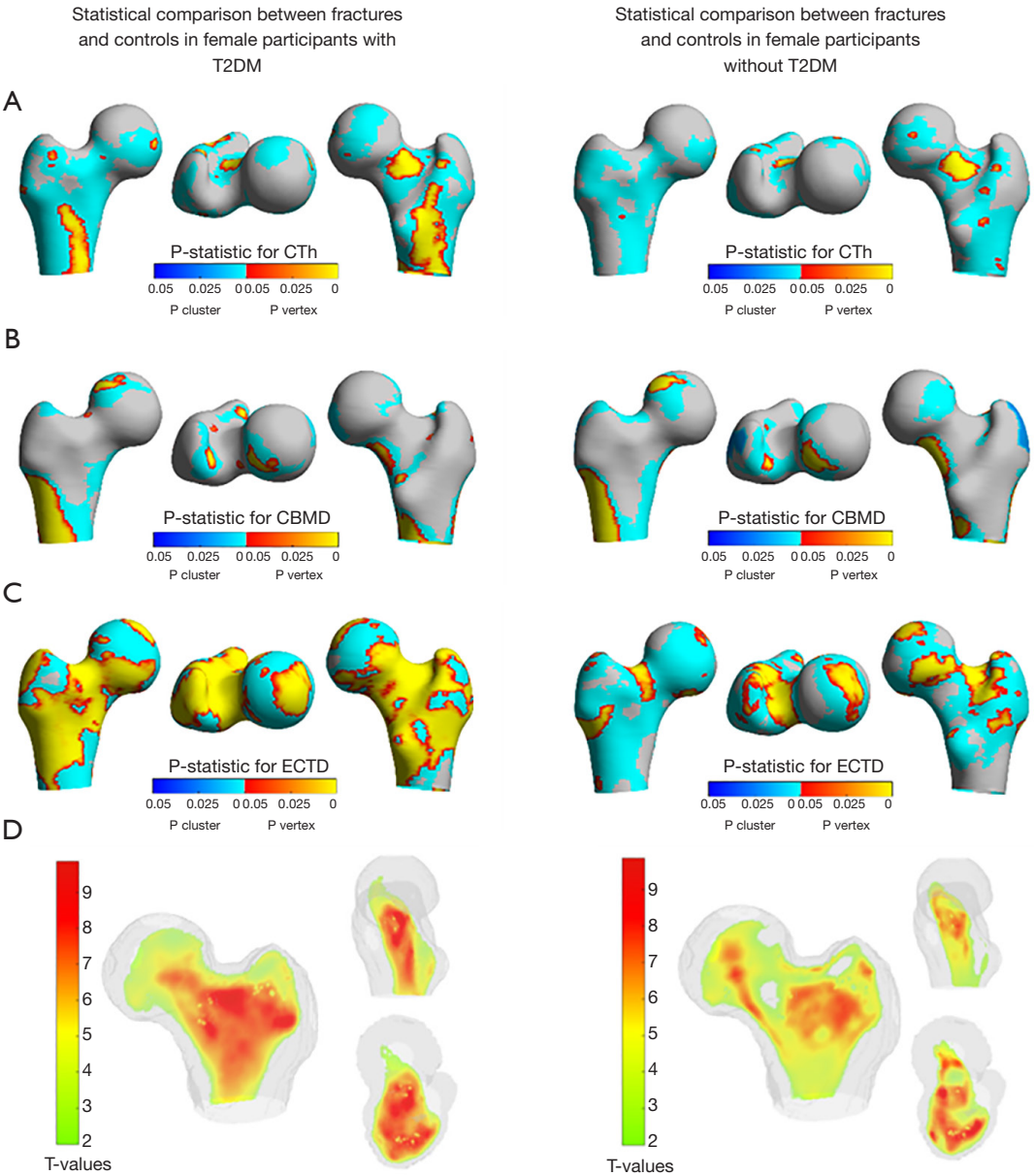

Figure 3 Comparisons of different bone properties between female hip fractures and controls with and without T2DM. The left-hand images were derived from participants with T2DM and the right-hand images were derived from participants without T2DM. (A) SPM T-maps from CTh comparisons; (B) SPM T-maps from CBMD comparisons; (C) SPM T-maps from ECTD comparisons; (D) VBM T-maps from vBMD comparisons. In parts A, B and C of these figures, the P-vertex results (yellow-orange colour map) show P values for vertex peaks, and the P-cluster results (cyan-blue colour map) show P values of connected clusters that exceed a P value threshold of 0.05. The color scale in D is based on the dynamic range of Student's *t*-values, where nonsignificant voxels have been rendered transparent and significant voxels assigned a degree of opacity based on its *t*-value. CBMD, cortical bone mineral density; CTh, cortical thickness; ECTD, endocortical trabecular bone mineral density; SPM, statistical parametric mapping; T2DM, type 2 diabetes mellitus; VBM, voxel-based morphometry; vBMD, volumetric bone mineral density.

Table 2 Quantitative results of focal patches of bone mapping

Variables	Hip fracture patients		Controls		P values	
	With T2DM [1]	Without T2DM [2]	With T2DM [3]	Without T2DM [4]	[1] *vs.* [3]	[2] *vs.* [4]
Male						
CTh_patch (mm)	0.9±0.2	1.0±0.1	1.3±0.2	1.2±0.2	0.0226	0.0147
CBMD_patch (mg/cm^3)	1,035.0±95.8	925.4±102.6	1,184.6±97.8	989.4±98.6	0.0250	0.0484
ECTD_patch (mg/cm^3)	70.8±25.0	77.8±30.4	141.7±31.3	137.3±33.1	0.0157	0.0126
VBM_patch (mg/cm^3)	129.4±26.6	144.8±34.3	187.4±35.8	198.5±35.6	0.0344	0.0286
Female						
CTh_patch (mm)	1.6±0.3	0.9±0.2	2.1±0.4	1.2±0.2	0.0141	0.0110
CBMD_patch (mg/cm^3)	1,143.4±93.4	1,142.1±61.7	1,262.8±98.4	1,260.0±86.2	0.0082	0.0070
ECTD_patch (mg/cm^3)	68.9±30.3	65.6±36.2	137.0±45.3	139.3±38.0	0.0062	0.0133
VBM_patch (mg/cm^3)	140.6±35.9	139.4±37.8	220.3±55.4	217.8±46.9	0.0211	0.0240

CBMD, cortical bone mineral density; CTh, cortical thickness; ECTD, endocortical trabecular bone mineral density; T2DM, type 2 diabetes mellitus; VBM, voxel-based morphometry.

underlying mechanisms are still unclear. Plenty of studies have shown that T2DM patients have higher or equivalent BMD compared to without T2DM patients, which does not explain the higher hip fracture risk for T2DM. Schwartz *et al.* estimated the sensitivity of Fracture Risk Algorithm (FRAX) in fracture prediction by analyzing three well-known study cohorts [Study of Osteoporotic Fractures (SOF), Osteoporotic Fractures in Men (MrOS), and Health, Aging, and Body Composition (Health ABC)], and found that women with T2DM tend to fracture at a higher T score (3). These findings indicate that DXA measurements alone do not reflect the complexity of underlying skeletal abnormalities in diabetes. Thus, it is essential to assess bone competence impairments by using advanced imaging methods such as the measurement of CTh and BMD of the cortical and trabecular compartments. Our results showed that the loss of ECTD in hip fracture patients with T2DM is different from the observation of differences between hip fracture patients and controls without T2DM (*Figures 2*,*3*). These results indicate that defects in average density in the trabecular compartment close to the cortex in T2DM patients might play an important role in increasing hip fracture risk. There is evidence showing that T2DM suppresses bone formation and is associated with negative effects on the mechanoenzyme properties of osteocytes (27-29). At a structural level, the accumulation of advanced glycation end (AGE) products under diabetic conditions has been proposed to alter collagen structure and contribute to impaired material properties (30). Interestingly, a recent study for hip fracture risk identification combining data from the Czech Republic and the UK found distinct patterns of ECTD linked to different fracture types, with focal reductions of around 50% ECTD in cases compared with controls (15). In another multi-trial analysis, the effects of Teriparatide (TPTD) over different treatment periods were confirmed by a statistically significant increase in ECTD between 18 and 24 months (31). By using HR-pQCT, a recent study showed that T2DM have poorer cortical bone values, namely lower cortical vBMD, reduced CTh, and higher cortical porosity of the radius (32). The negative effect of T2DM on cortical bone found in this HR-pQCT study supports our own findings. Thus, reduced ECTD may be a strong predictor of hip fractures in T2DM patients, and improving ECTD is therefore a valid target when considering strategies to reduce hip fractures.

The possible mechanisms include impaired bone quality (12) and increased fall risk. However, a recent study showed that T2DM females experienced long-term porosity increases at a rate similar to without T2DM (33). One of our main findings was that T2DM patients with and without hip fractures displayed a discordant proximal femoral vBMD spatial distribution, similar to the outcomes of lower integral vBMD at all femoral sites in T2DM patients with a history of fracture reported in a previous study (34).

Two previous studies (35,36) indicated that trabecular

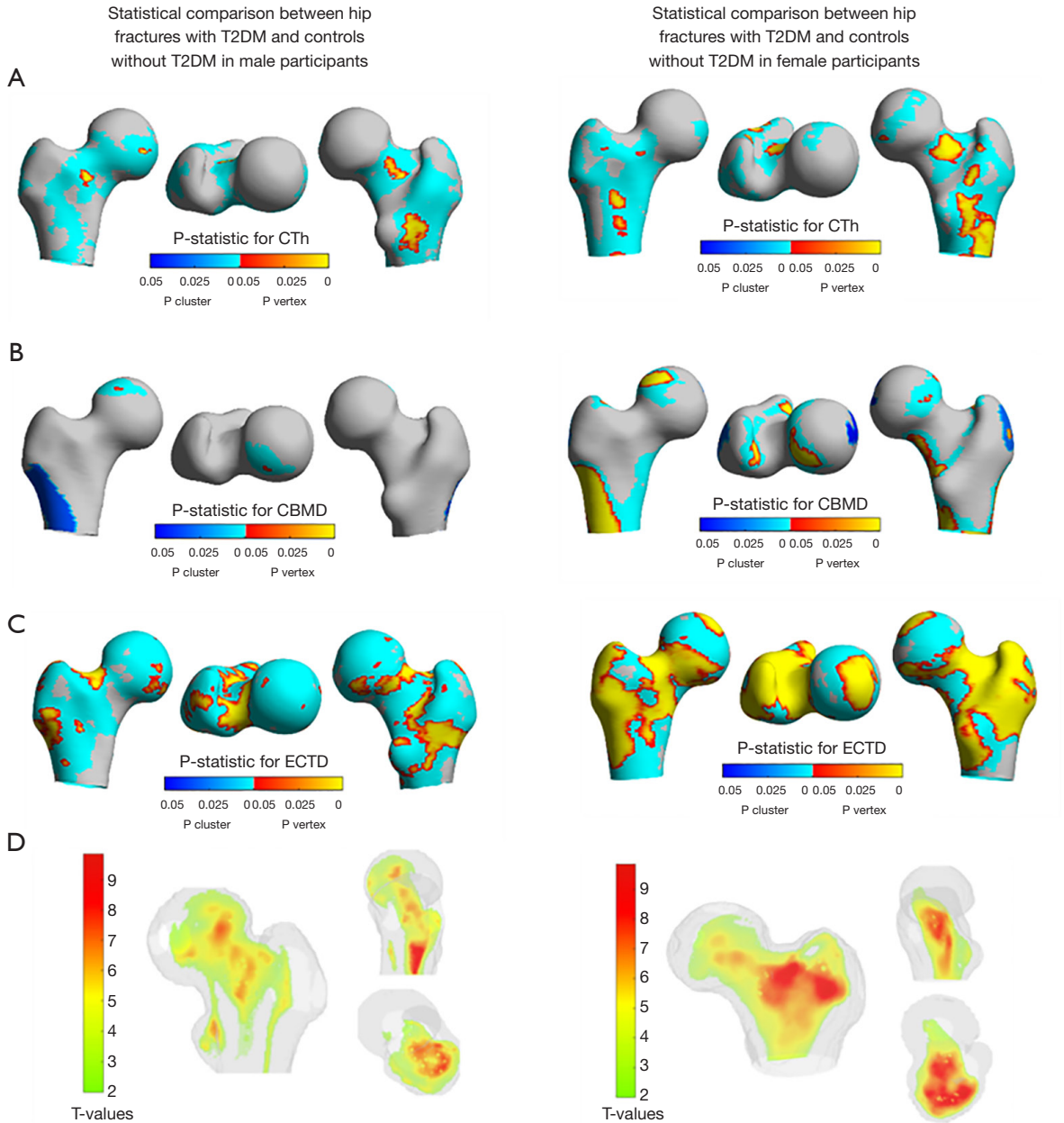

Figure 4 Comparisons of different bone properties between hip fractures with T2DM and controls without T2DM. (A) SPM T-maps from CTh comparisons; (B) SPM T-maps from CBMD comparisons; (C) SPM T-maps from ECTD comparisons; (D) VBM T-maps from vBMD comparisons. CBMD, cortical bone mineral density; CTh, cortical thickness; ECTD, endocortical trabecular bone mineral density; SPM, statistical parametric mapping; T2DM, type 2 diabetes mellitus; VBM, voxel-based morphometry; vBMD, volumetric bone mineral density.

bone mass and structure are intact and perhaps even enhanced, whereas the cortex is preferentially compromised in T2DM. These findings are significant because cortical bone accounts for 80% of the skeleton and fractures in diabetes frequently occur in cortical bone-rich areas (37). However, these observations were made at appendicular sites assessed via HR-pQCT. Our results confirm the importance of assessments of hip fracture risk in the cortical bone of the proximal femur in T2DM patients, especially elderly men [*Figure 4*; CBMD OR 0.06, 95% confidence interval (CI): 0.01, 0.27 for T2DM; OR 0.56, 95% CI: 0.37, 0.87 for without T2DM]. Interestingly, compared

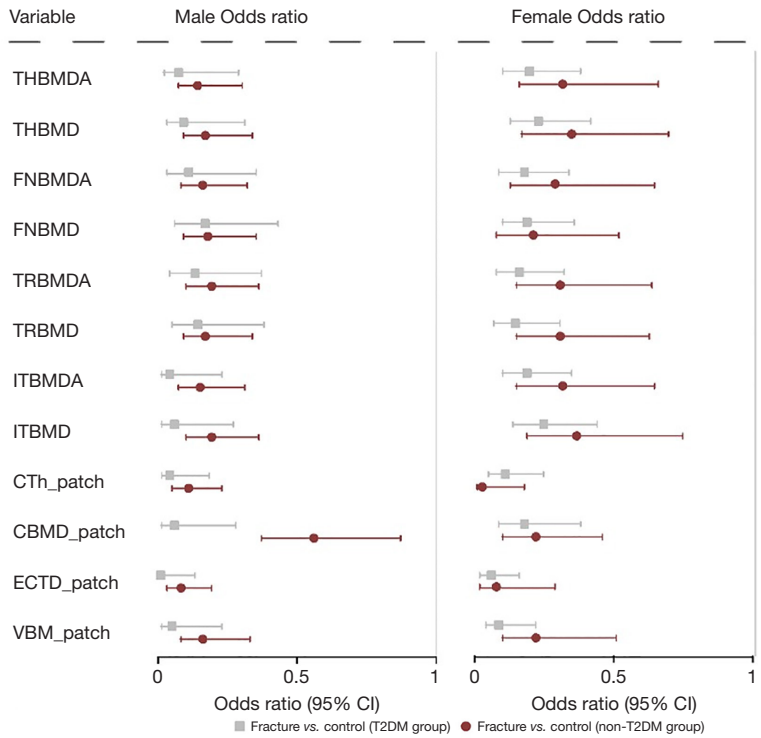

Figure 5 ORs with 95% CIs between fractures and controls with or without T2DM for different bone properties for hip fracture. The left-hand results are for the male population, and the right-hand images are for the female population. All ORs were adjusted for age, height and weight, respectively. P for interaction refers to testing whether ORs for each bone property differed by T2DM status. CBMD, cortical bone mineral density; CI, confidence interval; CTh, cortical thickness; ECTD, endocortical trabecular bone mineral density; FNBMD, femoral neck bone mineral density; FNBMDA, femoral neck areal bone mineral density; ITBMD, intertrochanter bone mineral density; ITBMDA, intertrochanter areal bone mineral density; OR, odds ratio; T2DM, type 2 diabetes mellitus; THBMD, total hip bone mineral density; THBMDA, total hip areal bone mineral density; TRBMD, trochanter bone mineral density; TRBMDA, trochanter areal bone mineral density; VBM, voxel-based morphometry.

to previous reports documenting that the percentage difference in CBMD is much smaller between hip fracture cases and controls compared to other SPM variables (15,38,39), the CBMD might contribute to hip fracture risk in the male diabetes population. In terms of SPM of CTh, the thinner cortices in regions in hip fracture patients in our study were in agreement with those published outcomes (38-40). Combined with these three studies, our study confirmed a focal patch of cortical bone thinning in the superior-anterior aspect of the FN in participants with hip fracture. These studies have identified spatial bone mapping a useful tool to build links between focal cortical defects and fracture risk. Further, CBM could identify the regions of increased thickness around the load-bearing bones in response to anti-osteoporosis treatment (41,42).

Previous studies (15,39) using statistical multiparametric mapping for hip fracture risk assessment have indicated the value of assessments of focal osteoporosis in clinical practice because hip fracture incidence is not fully explained by the diagnosis of osteoporosis using BMD measurements, and the identification of focal defects in bone might resolve this paradox. Furthermore, the identification of focal defects might help implement appropriate pharmacological or lifestyle interventions in clinical practice.

There are several limitations in this study. First, all measurements were taken after the hip fracture. However, as CT scans were taken within 48 h after fracture, for the purpose of this study, it is reasonable to assume that these participants had a high hip fracture risk. Thus, the comparisons between fracture cases (post-fracture) and controls should identify the characteristics of participants with high risk of hip fracture. Second, we

had no information about fall risk, which impedes further explanations of the relationship of hip fracture and diabetes. Third, clinical CT has poorer spatial resolution than HR-pQCT. As a result, measurements of CTh will tend to be overestimated and the range of measurements will be compressed. Similarly, measurements of cortical vBMD will be underestimated and the range of measurements expanded compared with HR-pQCT. However, HR-pQCT can only be applied to appendicular bones and not to the proximal femur. Another limitation is the significant age difference between the fracture cases and controls, as controls were younger than fracture cases. Age was a strong and independent predictor of hip fracture risk and the risk of hip fractures increased more than five times for people age 75–84 years (43). To address this issue, age was included as a co-variable in GLM and binomial logistic regression.

Conclusions

In conclusion, the spatial distribution of trabecular vBMD and focal areas of endocortical bone defect both result in increased risk of hip fracture in T2DM patients.

Acknowledgments

None.

Footnote

Reporting Checklist: The authors have completed the STROBE reporting checklist. Available at https://qims.amegroups.com/article/view/10.21037/qims-2025-560/rc

Data Sharing Statement: Available at https://qims.amegroups.com/article/view/10.21037/qims-2025-560/dss

Funding: This work was supported in part by the National Natural Science Foundation of China (Grant Nos. 82371957, 82371956, 81901718, 81771831, and 82072445), Beijing JST Research Fund (Code: 8002-903-02), Beijing Municipal Public Welfare Development and Reform Pilot Project for Medical Research Institutes (Code: JYY2023-8, JYY2023-11), Beijing Jishuitan Research Funding (Code: JSTYC202207), Beijing Hospitals Authority Youth Programme (Code: QML20200402), Beijing Physician Scientist Training Project (Code: BJPSTP-2024-08), Capital Medical University Outstanding Youth Talent Program (Category A) (No. A2413) and Suzhou Fundamental Research Program (No. SSD2024022).

Conflicts of Interest: All authors have completed the ICMJE uniform disclosure form (available at https://qims.amegroups.com/article/view/10.21037/qims-2025-560/coif). K.E. is a part-time employee of BioClinica, Inc. The other authors have no conflicts of interest to declare.

Ethical Statement: The authors are accountable for all aspects of the work in ensuring that questions related to the accuracy or integrity of any part of the work are appropriately investigated and resolved. The study was conducted in accordance with the Declaration of Helsinki and its subsequent amendments. The study was approved by institutional ethics committee of Beijing Jishuitan Hospital (No. 201512-02) and informed consent was taken from all the participants.

References

1. Saeedi P, Petersohn I, Salpea P, Malanda B, Karuranga S, Unwin N, Colagiuri S, Guariguata L, Motala AA, Ogurtsova K, Shaw JE, Bright D, Williams R; IDF Diabetes Atlas Committee. Global and regional diabetes prevalence estimates for 2019 and projections for 2030 and 2045: Results from the International Diabetes Federation Diabetes Atlas, 9(th) edition. Diabetes Res Clin Pract 2019;157:107843.
2. Reginster JY, Burlet N. Osteoporosis: a still increasing prevalence. Bone 2006;38:S4-9.
3. Schwartz AV, Vittinghoff E, Bauer DC, Hillier TA, Strotmeyer ES, Ensrud KE, Donaldson MG, Cauley JA, Harris TB, Koster A, Womack CR, Palermo L, Black DM; Study of Osteoporotic Fractures (SOF) Research Group; Osteoporotic Fractures in Men (MrOS) Research Group; Health, Aging, and Body Composition (Health ABC) Research Group. Association of BMD and FRAX score with risk of fracture in older adults with type 2 diabetes.

JAMA 2011;305:2184-92.
4. Oei L, Zillikens MC, Dehghan A, Buitendijk GH, Castaño-Betancourt MC, Estrada K, Stolk L, Oei EH, van Meurs JB, Janssen JA, Hofman A, van Leeuwen JP, Witteman JC, Pols HA, Uitterlinden AG, Klaver CC, Franco OH, Rivadeneira F. High bone mineral density and fracture risk in type 2 diabetes as skeletal complications of inadequate glucose control: the Rotterdam Study. Diabetes Care 2013;36:1619-28.
5. Ma L, Oei L, Jiang L, Estrada K, Chen H, Wang Z, Yu Q, Zillikens MC, Gao X, Rivadeneira F. Association between bone mineral density and type 2 diabetes mellitus: a meta-analysis of observational studies. Eur J Epidemiol 2012;27:319-32.
6. Wang L, Zhao K, Zha X, Ran L, Su H, Yang Y, Shuang Q, Liu Y, Xu L, Blake GM, Cheng X, Engelke K, Vlug A. Hyperglycemia Is Not Associated With Higher Volumetric BMD in a Chinese Health Check-up Cohort. Front Endocrinol (Lausanne) 2021;12:794066.
7. Ferrari SL, Abrahamsen B, Napoli N, Akesson K, Chandran M, Eastell R, El-Hajj Fuleihan G, Josse R, Kendler DL, Kraenzlin M, Suzuki A, Pierroz DD, Schwartz AV, Leslie WD; Bone and Diabetes Working Group of IOF. Diagnosis and management of bone fragility in diabetes: an emerging challenge. Osteoporos Int 2018;29:2585-96.
8. Chen HF, Ho CA, Li CY. Increased risks of hip fracture in diabetic patients of Taiwan: a population-based study. Diabetes Care 2008;31:75-80.
9. Schwartz AV, Sellmeyer DE, Ensrud KE, Cauley JA, Tabor HK, Schreiner PJ, Jamal SA, Black DM, Cummings SR; Study of Osteoporotic Features Research Group. Older women with diabetes have an increased risk of fracture: a prospective study. J Clin Endocrinol Metab 2001;86:32-8.
10. Shanbhogue VV, Mitchell DM, Rosen CJ, Bouxsein ML. Type 2 diabetes and the skeleton: new insights into sweet bones. Lancet Diabetes Endocrinol 2016;4:159-73.
11. Hamann C, Kirschner S, Günther KP, Hofbauer LC. Bone, sweet bone--osteoporotic fractures in diabetes mellitus. Nat Rev Endocrinol 2012;8:297-305.
12. Samelson EJ, Demissie S, Cupples LA, Zhang X, Xu H, Liu CT, Boyd SK, McLean RR, Broe KE, Kiel DP, Bouxsein ML. Diabetes and Deficits in Cortical Bone Density, Microarchitecture, and Bone Size: Framingham HR-pQCT Study. J Bone Miner Res 2018;33:54-62.
13. Nilsson AG, Sundh D, Johansson L, Nilsson M, Mellström D, Rudäng R, Zoulakis M, Wallander M, Darelid A, Lorentzon M. Type 2 Diabetes Mellitus Is Associated With Better Bone Microarchitecture But Lower Bone Material Strength and Poorer Physical Function in Elderly Women: A Population-Based Study. J Bone Miner Res 2017;32:1062-71.
14. Engelke K. Assessment of bone quality and strength with new technologies. Curr Opin Endocrinol Diabetes Obes 2012;19:474-82.
15. Poole KES, Skingle L, Gee AH, Turmezei TD, Johannesdottir F, Blesic K, Rose C, Vindlacheruvu M, Donell S, Vaculik J, Dungl P, Horak M, Stepan JJ, Reeve J, Treece GM. Focal osteoporosis defects play a key role in hip fracture. Bone 2017;94:124-34.
16. Carballido-Gamio J, Marques EA, Sigurdsson S, Siggeirsdottir K, Jensen A, Sigurdsson G, Aspelund T, Gudnason V, Lang TF, Harris TB. Male-female spatio-temporal differences of age-related bone changes show faster bone deterioration in older women at femoral regions associated with incident hip fracture. J Bone Miner Res 2024;39:1443-53.
17. Treece G, Gee A. Cortical Bone Mapping: Measurement and Statistical Analysis of Localised Skeletal Changes. Curr Osteoporos Rep 2018;16:617-25.
18. Wang L, Museyko O, Su Y, Brown K, Yang R, Zhang Y, Duanmu Y, Guo Z, Zhang W, Yan D, Cheng X, Engelke K. QCT of the femur: Comparison between QCTPro CTXA and MIAF Femur. Bone 2019;120:262-70.
19. Su YB, Wang L, Wu XB, Yi C, Yang MH, Yan D, Cheng KB, Cheng XG. The spatial differences in bone mineral density and hip structure between low-energy femoral neck and trochanteric fractures in elderly Chinese using quantitative computed tomography. Bone 2019;124:62-8.
20. Wang L, Yin L, Yang M, Ge Y, Liu Y, Su Y, et al. Muscle density is an independent risk factor of second hip fracture: a prospective cohort study. J Cachexia Sarcopenia Muscle 2022;13:1927-37.
21. Cheng X, Wang L, Wang Q, Ma Y, Su Y, Li K. Validation of quantitative computed tomography-derived areal bone mineral density with dual energy X-ray absorptiometry in an elderly Chinese population. Chin Med J (Engl) 2014;127:1445-9.
22. Wang L, Yin L, Zhao Y, Su Y, Sun W, Liu Y, Yang M, Yu A, Blake GM, Cheng X, Wu X, Veldhuis A, Engelke K. Muscle density discriminates hip fracture better than computed tomography X-ray absorptiometry hip areal bone mineral density. J Cachexia Sarcopenia Muscle 2020;11:1799-812.
23. Museyko O, Bousson V, Adams J, Laredo J-, Engelke K. QCT of the proximal femur--which parameters should

be measured to discriminate hip fracture? Osteoporos Int 2016;27:1137-47.
24. Myronenko A, Song X. Point set registration: coherent point drift. IEEE Trans Pattern Anal Mach Intell 2010;32:2262-75.
25. Whitwell JL. Voxel-based morphometry: an automated technique for assessing structural changes in the brain. J Neurosci 2009;29:9661-4.
26. Gee AH, Treece GM. Systematic misregistration and the statistical analysis of surface data. Med Image Anal 2014;18:385-93.
27. Manavalan JS, Cremers S, Dempster DW, Zhou H, Dworakowski E, Kode A, Kousteni S, Rubin MR. Circulating osteogenic precursor cells in type 2 diabetes mellitus. J Clin Endocrinol Metab 2012;97:3240-50.
28. Jiajue R, Jiang Y, Wang O, Li M, Xing X, Cui L, Yin J, Xu L, Xia W. Suppressed bone turnover was associated with increased osteoporotic fracture risks in non-obese postmenopausal Chinese women with type 2 diabetes mellitus. Osteoporos Int 2014;25:1999-2005.
29. Napoli N, Strollo R, Defeudis G, Leto G, Moretti C, Zampetti S, D'Onofrio L, Campagna G, Palermo A, Greto V, Manfrini S, Hawa MI, Leslie RD, Pozzilli P, Buzzetti R; NIRAD (NIRAD 10) and Action LADA Study Groups. Serum Sclerostin and Bone Turnover in Latent Autoimmune Diabetes in Adults. J Clin Endocrinol Metab 2018;103:1921-8.
30. Picke AK, Campbell G, Napoli N, Hofbauer LC, Rauner M. Update on the impact of type 2 diabetes mellitus on bone metabolism and material properties. Endocr Connect 2019;8:R55-70.
31. Whitmarsh T, Treece GM, Gee AH, Poole KE. The Effects on the Femoral Cortex of a 24 Month Treatment Compared to an 18 Month Treatment with Teriparatide: A Multi-Trial Retrospective Analysis. PLoS One 2016;11:e0147722.
32. de Waard EAC, de Jong JJA, Koster A, Savelberg HHCM, van Geel TA, Houben AJHM, Schram MT, Dagnelie PC, van der Kallen CJ, Sep SJS, Stehouwer CDA, Schaper NC, Berendschot TTJM, Schouten JSAG, Geusens PPMM, van den Bergh JPW. The association between diabetes status, HbA1c, diabetes duration, microvascular disease, and bone quality of the distal radius and tibia as measured with high-resolution peripheral quantitative computed tomography-The Maastricht Study. Osteoporos Int 2018;29:2725-38.
33. Heilmeier U, Joseph GB, Pasco C, Dinh N, Torabi S, Darakananda K, Youm J, Carballido-Gamio J, Burghardt AJ, Link TM, Kazakia GJ. Longitudinal Evolution of Bone Microarchitecture and Bone Strength in Type 2 Diabetic Postmenopausal Women With and Without History of Fragility Fractures-A 5-Year Follow-Up Study Using High Resolution Peripheral Quantitative Computed Tomography. Front Endocrinol (Lausanne) 2021;12:599316.
34. Heilmeier U, Carpenter DR, Patsch JM, Harnish R, Joseph GB, Burghardt AJ, Baum T, Schwartz AV, Lang TF, Link TM. Volumetric femoral BMD, bone geometry, and serum sclerostin levels differ between type 2 diabetic postmenopausal women with and without fragility fractures. Osteoporos Int 2015;26:1283-93.
35. Petit MA, Paudel ML, Taylor BC, Hughes JM, Strotmeyer ES, Schwartz AV, Cauley JA, Zmuda JM, Hoffman AR, Ensrud KE; Osteoporotic Fractures in Men (MrOs) Study Group. Bone mass and strength in older men with type 2 diabetes: the Osteoporotic Fractures in Men Study. J Bone Miner Res 2010;25:285-91.
36. Burghardt AJ, Issever AS, Schwartz AV, Davis KA, Masharani U, Majumdar S, Link TM. High-resolution peripheral quantitative computed tomographic imaging of cortical and trabecular bone microarchitecture in patients with type 2 diabetes mellitus. J Clin Endocrinol Metab 2010;95:5045-55.
37. Leslie WD, Rubin MR, Schwartz AV, Kanis JA. Type 2 diabetes and bone. J Bone Miner Res 2012;27:2231-7.
38. Treece GM, Gee AH, Tonkin C, Ewing SK, Cawthon PM, Black DM, Poole KE; Osteoporotic Fractures in Men (MrOS) Study. Predicting Hip Fracture Type With Cortical Bone Mapping (CBM) in the Osteoporotic Fractures in Men (MrOS) Study. J Bone Miner Res 2015;30:2067-77.
39. Yu A, Carballido-Gamio J, Wang L, Lang TF, Su Y, Wu X, Wang M, Wei J, Yi C, Cheng X. Spatial Differences in the Distribution of Bone Between Femoral Neck and Trochanteric Fractures. J Bone Miner Res 2017;32:1672-80.
40. Poole KE, Treece GM, Mayhew PM, Vaculík J, Dungl P, Horák M, Štěpán JJ, Gee AH. Cortical thickness mapping to identify focal osteoporosis in patients with hip fracture. PLoS One 2012;7:e38466.
41. Whitmarsh T, Treece GM, Gee AH, Poole KE. Mapping Bone Changes at the Proximal Femoral Cortex of Postmenopausal Women in Response to Alendronate and Teriparatide Alone, Combined or Sequentially. J Bone Miner Res 2015;30:1309-18.
42. Poole KE, Treece GM, Pearson RA, Gee AH, Bolognese

MA, Brown JP, Goemaere S, Grauer A, Hanley DA, Mautalen C, Recknor C, Yang YC, Rojeski M, Libanati C, Whitmarsh T. Romosozumab Enhances Vertebral Bone Structure in Women With Low Bone Density. J Bone Miner Res 2022;37:256-64.
43. Finsterwald M, Sidelnikov E, Orav EJ, Dawson-Hughes B, Theiler R, Egli A, Platz A, Simmen HP, Meier C, Grob D, Beck S, Stähelin HB, Bischoff-Ferrari HA. Gender-specific hip fracture risk in community-dwelling and institutionalized seniors age 65 years and older. Osteoporos Int 2014;25:167-76.

Cite this article as: Yuan Y, Zhang R, Yang M, Xia W, Su Y, Jian J, Liu Y, Guo Z, Zhao X, Zhu S, Cheng X, Wu X, Blake GM, Vlug A, Engelke K, Gao X, Wang L. Focal bone defects in type 2 diabetes mellitus patients with acute hip fractures. Quant Imaging Med Surg 2025;15(10):9400-9415. doi: 10.21037/qims-2025-560